Petrov-Galerkin Finite Element Stabilization for Two-Phase Flows

MICHELE GIORDANO and VINICIO MAGI
Department of Environmental Engineering and Physics
University of Basilicata
Via dell'Ateneo Lucano, Potenza, 85100
ITALY

Abstract: - This paper presents a finite element model for incompressible laminar two-phase flows. A two-fluid model, describing the laminar non-equilibrium flow of two incompressible phases, is discretized by means of a properly designed Streamline Upwind Petrov-Galerkin (SUPG) finite element procedure. Such a procedure is consistent with a continuous pressure equation. The design and the implementation of the algorithm are presented together with its validation through a comparison with results available in the literature.

Key-Words: - finite element method, two-phase flow, two-fluid model, SUPG

1 Introduction

The finite element (FE) methodology is a numerical approach to solve approximately a partial differential equation. There are some advantages in using the FE method. First, there are no restrictions on the mesh used to discretize the domain, so very complex geometries can be easily handled. A characteristic of the method is that it does not attempt to solve a partial differential equation (PDE) itself, but it rather searches a solution for an integral weak formulation of the PDE. This integral form is most commonly obtained from a weighted residual formulation. An advantage coming from this particular approach is that there is a common and widespread knowledge on the possibilities to solve stabilization problems [1, 2, 3]. Starting from consolidated techniques applied to single-phase flow, the present work focus on the achievement of a properly designed finite element based numerical stabilization of a two-phase flow model.

Two-phase flows are encountered in a wide variety of engineering applications ranging from power generation and conversion to biological flows. This leads to a general interest in two-phase models [4] that may describe the behaviour of these systems. A compromise between the complexity of the model and its suitability to the physics of the problem is reached in the two-fluid models, obtained through space (or time or space-time or ensemble) averages of the Navier-Stokes equations. These averaged models describe the two-phase systems from a macroscopic point of view, allowing a more engineering oriented analysis.

In the following, the governing equations describing the two-phase flow and the stabilized finite element approach are given. Then, some test cases, to validate the proposed methodology, are presented.

2 Two-phase model

The governing equations, describing the behaviour of the two-phase flow, are presented in this section.

2.1 Basic Concepts

The adopted model is an Eulerian-Eulerian one, since both phases are treated as *continua*. Moreover, a pressure equilibrium between the phases is assumed, leading to the following relation:

$$p_l = p_g = p \tag{1}$$

where p is the pressure, and the subscripts l and g are referred to the primary and the secondary phases, respectively.

Since the phases are considered as interpenetrating, each of them occupies a well-defined volume of space. The volume V_q of the generic phase q is defined by

$$V_q = \int_\Omega \alpha_q d\Omega \tag{2}$$

where α_q is the phasic volume fraction, representing the volume fraction occupied by the phase q in the whole domain Ω. The summation of the phase volumes must recover the whole domain, so the volume fractions of the phases are linked by the following relation:

$$\alpha_g + \alpha_l = 1 \tag{3}$$

Equation (3) represents the fundamental constitutive law for the volume fractions.

2.2 Mass Conservation

The two-phase flow model must guarantee the conservation of mass and momentum.

Referring to the continuity equation of the generic phase q, with the hypothesis of incompressibility, one can write:

$$\frac{\partial \alpha_q}{\partial t} + \nabla \cdot (\alpha_q \vec{u}_q) = 0 \tag{4}$$

where ρ_q and $\vec{u}_q$ are the density and the velocity of the phase, respectively.

2.3 Momentum Conservation

Without body forces, the momentum balance for the generic phase q yields

$$\frac{\partial \vec{u}_q}{\partial t} + \vec{u}_q \cdot \nabla \vec{u}_q = \vec{F}_{p,q} + \vec{F}_{v,q} + \vec{F}_{d,q} \tag{5}$$

where $\vec{F}_{p,q}$ is representative of the pressure contribution, $\vec{F}_{v,q}$ of the viscous force, and $\vec{F}_{d,q}$ of the drag force, i.e. the interaction between the phases.

The pressure and the viscous force contribution are equal to

$$\vec{F}_{p,q} = -\frac{1}{\rho_q} \nabla p \qquad \vec{F}_{v,q} = \frac{1}{\rho_q \alpha_q} \nabla \cdot \left(\alpha_q \overline{\overline{\tau}}_q \right) \tag{6}$$

with the stress tensor written as

$$\overline{\overline{\tau}}_q = \mu_q \left(\nabla \vec{u}_q + \nabla \vec{u}_q^T \right) \tag{7}$$

where μ_q is the shear viscosity and the superscript symbol T denotes the transpose of $\nabla \vec{u}_q$.

Referring to the primary phase l and to the secondary phase g, the drag force can be written as

$$\vec{F}_{d,l} = \frac{3}{4} \frac{C_D}{d_g \rho_l} \alpha_g \rho |\vec{u}_g - \vec{u}_l| \left(\vec{u}_g - \vec{u}_l \right) \tag{8}$$

where C_D is the drag coefficient, d_g is the diameter of the bubbles of the secondary phase and ρ is the mixture density defined as

$$\rho = \alpha_l \rho_l + \alpha_g \rho_g \tag{9}$$

2.4 System of Equations

Referring to the primary phase as l and to the secondary phase as g, the chosen set of variables is done by

$$\boldsymbol{U} = \left(p \;\; u_l \;\; v_l \;\; \alpha_g \;\; u_g \;\; v_g \right)^T \tag{10}$$

Hence, the final system of equations is made of six equations: five equations are given by the conservation of the momentum for each phase and the continuity equation written for the secondary phase volume fraction. The remaining continuity equation is not needed because of the costitutive relation (3).

The sixth equation, needed for the pressure evaluation, is obtained from the conservation of the total volume ($\sum_{q=l,g} \alpha_q = 1$) applied to the mass conservation equations:

$$\sum_{q=l,g} \nabla \cdot (\alpha_q \vec{u}_q) = 0 \tag{11}$$

Then, for this equation, the artificial compressibility formulation is adopted: a pressure time derivative is introduced to enhance robustness for steady simulations [5]. The re-arranged equation for the pressure is

$$\frac{1}{\rho c^2} \frac{\partial p}{\partial t} + \nabla \cdot ((1 - \alpha_g) \vec{u}_l) + \nabla \cdot (\alpha_g \vec{u}_g) = 0 \tag{12}$$

where c is a reference velocity and ρ is the mixture density.

3 Finite element approach

The discretization of the governing equations is made through a Galerkin finite element approach with $P1$ basis functions for all the variables [6]. By means of this approach, piecewise linear functions are used both for the basis and the weighting functions. In addition, a Petrov-Galerkin stabilization is adopted.

3.1 Galerkin Formulation

The governing equations can be written as a system of equations in terms of the chosen set of variables $\boldsymbol{U}$

$$\mathcal{L}(\boldsymbol{U}) = \boldsymbol{A}_0 \boldsymbol{U}_{,t} + \boldsymbol{F}^{adv}_{i,i} - \boldsymbol{F}^{diff}_{i,i} = \boldsymbol{S} \tag{13}$$

where $\boldsymbol{F}^{adv}_{i,i} = \boldsymbol{A}_i \boldsymbol{U}_{,i}$ is the advective contribution, $\boldsymbol{F}^{diff}_{i,i}$ is the diffusive contribution, and $\boldsymbol{S}$ represents the source term.

Introducing the trial solution space $\mathcal{V}_h$, and the weighting solution space $\mathcal{W}_h$, the weak form of (13) reads as find $\boldsymbol{U} \in \mathcal{V}_h$ such that $\forall\, \boldsymbol{W} \in \mathcal{W}_h$

$$\int_\Omega (\boldsymbol{W} \cdot \boldsymbol{A}_0 \boldsymbol{U}_{,t} - \boldsymbol{W}_{,i} \cdot \boldsymbol{F}^{adv}_i + \boldsymbol{W}_{,i} \cdot \boldsymbol{F}^{diff}_i - \boldsymbol{W} \cdot \boldsymbol{S})\, d\Omega - \int_\Gamma \boldsymbol{W} \cdot (-\boldsymbol{F}^{adv}_i + \boldsymbol{F}^{diff}_i)\, d\Gamma = 0 \tag{14}$$

where Ω is the spatial domain and Γ represents its boundaries.

3.2 SUPG Formulation

The stabilization is done following a Streamline Upwind Petrov-Galerkin (SUPG) procedure applied to advection-diffusion systems. The new integral equation is

$$\int_\Omega (\boldsymbol{W}\cdot\boldsymbol{A}_0\boldsymbol{U}_{,t} - \boldsymbol{W}_{,i}\cdot\boldsymbol{F}_i^{adv} + \boldsymbol{W}_{,i}\cdot\boldsymbol{F}_i^{diff} - \boldsymbol{W}\cdot\boldsymbol{S})\, d\Omega - \int_\Gamma \boldsymbol{W}\cdot(-\boldsymbol{F}_i^{adv} + \boldsymbol{F}_i^{diff})\, d\Gamma + \boldsymbol{ST}_{supg} = 0 \quad (15)$$

where

$$\boldsymbol{ST}_{supg} = \sum_{e=1}^{n_{el}} \int_{\Omega_e} \boldsymbol{A}_i^T \boldsymbol{U}_{,i}\cdot\boldsymbol{\tau}(\mathcal{L}(\boldsymbol{U}) - \boldsymbol{S}) d\Omega \quad (16)$$

In the above formula Ω_e is one of the n_{el} elements in which the domain is divided into, and $\boldsymbol{\tau}$ represents the matrix of the intrinsic time scales of the stabilizing operator.

The choice of $\boldsymbol{\tau}$ is not trivial; here a simple diagonal matrix is adopted

$$\boldsymbol{\tau} = diag(\tau_p, \tau_m, \tau_m, \tau_\alpha, \tau_m, \tau_m) \quad (17)$$

with

$$\tau_p = \tau_m = \tau_\alpha \quad (18)$$

and the choice of τ_m is done by following some definitions available in the literature [2, 7].

4 Numerical Results

In this section, the results of the numerical simulation of the two-phase, laminar, steady flow in a channel and in a T-junction are presented.

4.1 Two-Phase Flow in a Channel

The first test case concerns with the two-dimensional two-phase laminar flow in a channel. Nevertheless this example presents a relatively simple geometry, the presence of two phases renders the flow much more complex than the single phase one. In the present calculation no interactions between the two phases are considered (*i.e.* zero drag force).

The simulation is obtained by imposing the velocity at the inlet and setting uniform zero pressure at the outlet, so that the pressure at the inlet is evaluated from the computation. The other boundaries are treated as no-slip walls. The chosen inlet velocity profile is set to be uniform. The geometry is shown in Fig. 1. For the given geometry and velocity u at the inlet, the Reynolds number is

$$Re = \frac{ud}{\nu} \quad (19)$$

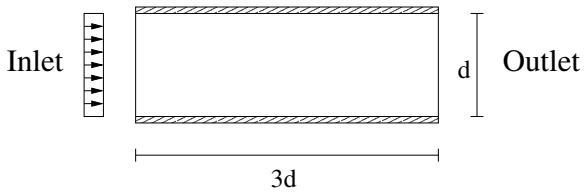

Figure 1: *Two-phase flow in a channel - geometry.*

Reynolds Number	$Re_1 = 100$	$Re_2 = 100$
Kinematic Viscosity	$\mu_1 = 0.01$	$\mu_2 = 0.01$
Density	$\rho_1 = 1.0$	$\rho_2 = 0.5$
Inlet Volume Fraction	$\alpha_1 = 0.5$	$\alpha_2 = 0.5$

Table 1: *Two-phase flow in a channel - physical properties.*

where ν is the kinematic viscosity. Table 1 presents the physical properties of the two phases.

Different grids are considered: the coarsest grid consists of 1699 nodes and 3236 elements, and the finest one consists of 33965 nodes and 67168 elements. The grids present a boundary layer refinement.

The comparison with the reference results in [8] is done for the horizontal velocity profiles of both phases along the center-line of the channel. The results, as seen in Fig. 2, show a quite good agreement with the reference solution. In Fig. 3 the dependency of the solution from the grid is also shown. Further comparisons are made for the pressure and the volume fraction. Figure 4 shows the static pressure along the centerline of the channel for the two different solutions. Regarding the volume fraction, the comparison is made through the values obtained along a vertical cut at $x = 2.5d$. The results are shown in Fig. 5.

4.2 Two-Phase Flow in a T-Junction

The aim of this test case is to demonstrate the correctness of the implementation of the model and its accuracy for relatively complex flow patterns due to phase separation and mixing. The solution obtained is again compared with the one presented in [8]. The geometry of the problem is shown in Fig. 6.

The simulation is carried out setting the same uniform velocity u at the two inlets and zero pressure at the outlet. The remaining boundaries are treated as no-slip walls. For the given geometry and velocity u at the inlet, the Reynolds number is defined as

$$Re = \frac{ud}{\nu} \quad (20)$$

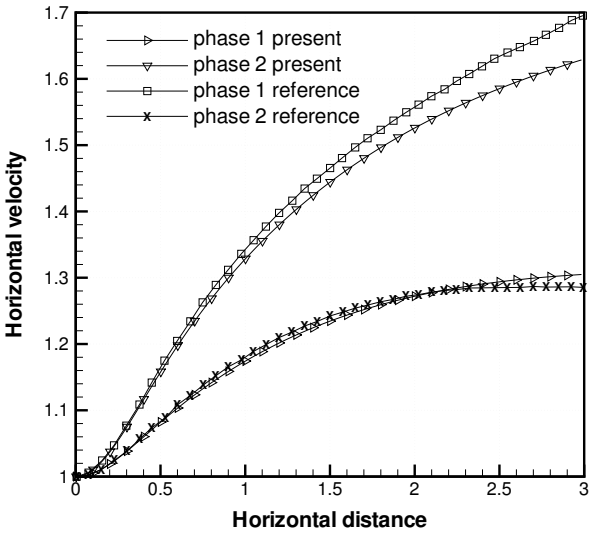

Figure 2: *Two-phase flow in a channel - comparison for horizontal velocity profiles along y=0.5d between [8] and the present solution.*

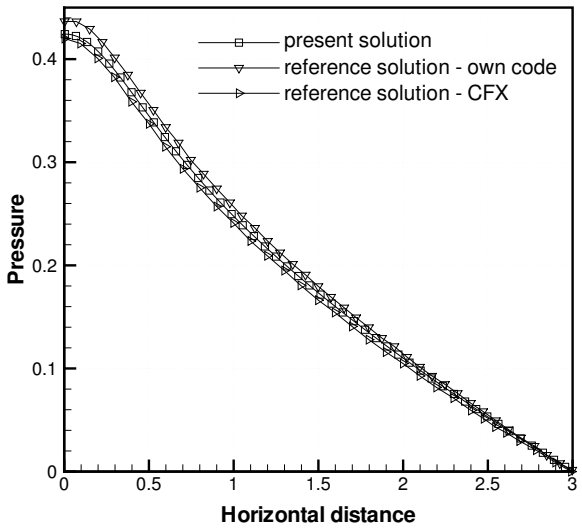

Figure 4: *Two-phase flow in a channel - comparison between the present and the reference solution [8] for the pressure profiles along $y = 0.5d$.*

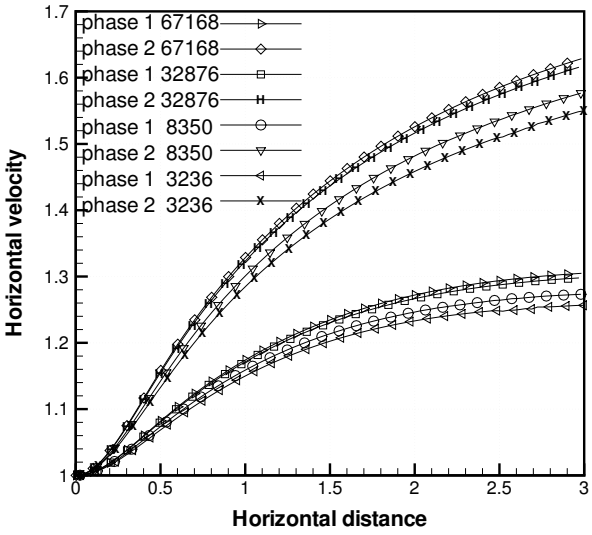

Figure 3: *Two-phase flow in a channel - comparison for horizontal velocity profiles along y=0.5d in the present solution with different grids.*

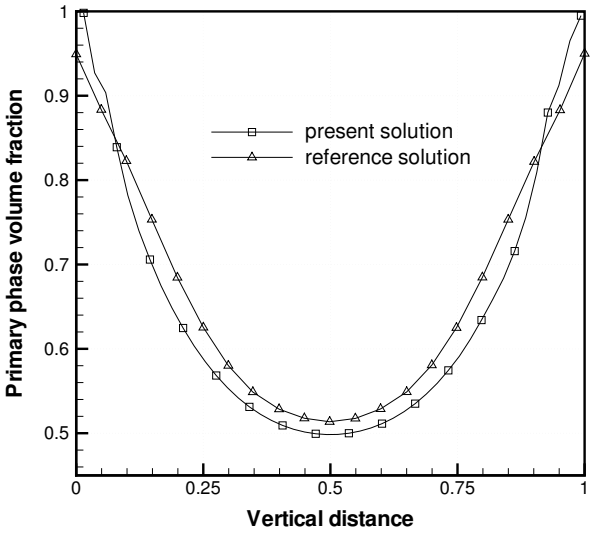

Figure 5: *Two-phase flow in a channel - the present and the reference solution [8] for the primary phase volume fraction profiles along $x = 2.5d$.*

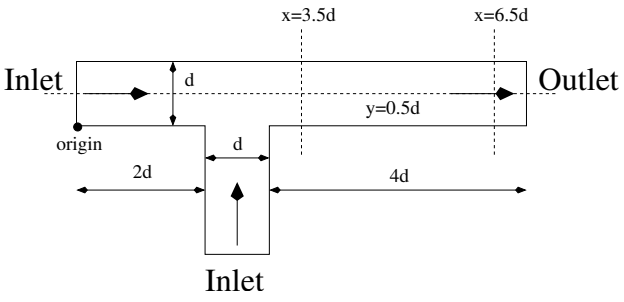

Figure 6: *Two-phase flow in a T-junction - geometry of the problem.*

On Tab. 2 the value of the physical properties of both phases are shown.

Reynolds Number	$Re_1 = 100$	$Re_2 = 75$
Kinematic Viscosity	$\mu_1 = 0.01$	$\mu_2 = 0.0066$
20 Density	$\rho_1 = 1.0$	$\rho_2 = 0.5$
Inlet Volume Fraction	$\alpha_1 = 0.5$	$\alpha_2 = 0.5$

Table 2: *Two-phase flow in a channel - physical properties.*

Different unstructured grids are considered for the simulation: the coarsest grid consists of 1676 nodes and 3158 elements, and the finest one consists of 9981 nodes and 19468 elements. The grids present a boundary layer refinement, to better reproduce the behaviour of the flow near the corners. In order to be as close as possible to the solution of [8], the same drag force parameters are used. In particular

$$C_D = 1 \qquad \text{and} \qquad d_g = 0.1 \tag{21}$$

The comparison with the reference results [8] is made by plotting the horizontal and vertical velocity profiles along the center-line of the main channel of the T-junction. The results are shown in Fig. 7. The velocity plotted are not referred to a specific phase, since, due to the presence of the drag force, the phases have the same components of velocity. Good agreement is achieved with the reference solution. In Fig. 8 the sensitivity of the solution from the grid is also shown. Regarding the volume fraction, the comparison is made through the values obtained along two different cuts, at $x = 3.5d$ and $x = 6.5d$. Figures 9-10 show the results from [8] and the present solution. The agreement between the two solutions is less good respect to the one obtained for the velocity profiles. Nevertheless the maximum value is comparable, some differences are located especially near the walls.

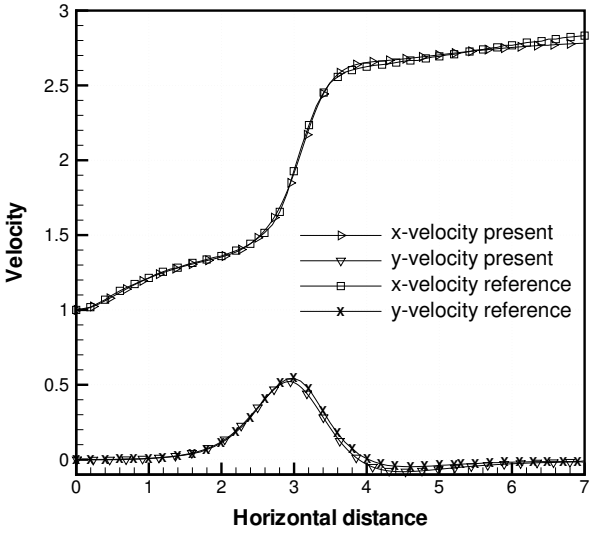

Figure 7: *Two-phase flow in a T-junction - comparison for the velocity profiles along y=0.5d between [8] and the present solution.*

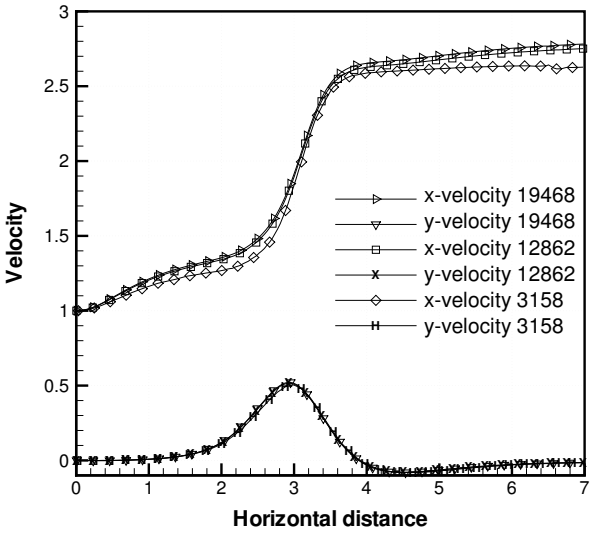

Figure 8: *Two-phase flow in a T-junction - comparison for the velocity profiles along y=0.5d in the present solution with different grids.*

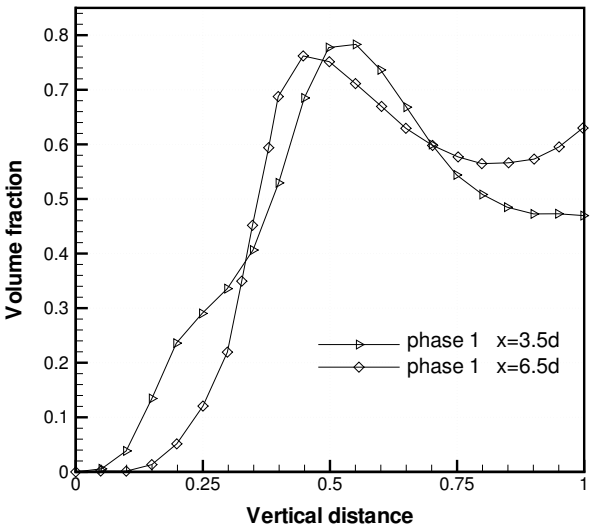

Figure 9: *Two-phase flow in a T-junction - primary phase volume fraction profiles along x=3.5d and x=6.5d in [8].*

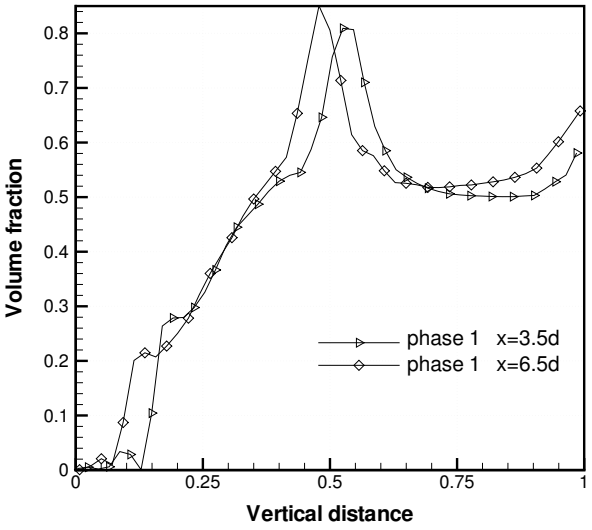

Figure 10: *Two-phase flow in a T-junction - primary phase volume fraction profiles along x=3.5d and x=6.5d in the present solution.*

5 Conclusions

This work dealt with the use of a Galerkin SUPG FE formulation for two phase-flows.

After the description of the two-phase flow model, the strategy to achieve the discretization and the stabilization of the set of equations has been presented. The resulting system of equations has been discretized as an advective-diffusive system, so that a SUPG stabilization has been performed, considering the advective matrice contributions. The accuracy of the method has been proved by comparing the results obtained, using multiple meshes, for the channel and the T-junction flow problems with the ones of [8].

The results obtained highlight how the choice of this approach is very promising in the two-phase flow treatement. They also suggest a better stabilization is needed in the boundary layer region, thus leading to the introduction of a discontinuity capturing operator, acting in this region.

References

[1] Hughes T. J. R., Franca L. P., and Balestra M., A new finite element formulation for computational fluid dynamics: V. Circumventing the Babuska-Brezzi condition: a stable Petrov-Galerkin formulation of the Stokes problem accomodating equal-order interpolations, *Computer Methods in Applied Mechanics and Engineering*, Vol.59, 1986, pp. 85-99.

[2] Hughes T. J. R., Mallet M. and Mizukami A., A new finite element formulation for computational fluid dynamics: II. Beyond SUPG, *Computer Methods in Applied Mechanics and Engineering*, Vol.54, 1986, pp. 341-355.

[3] Mizukami A., An implementation of the Streamline-Upwind/Petrov-Galerkin method for linear triangular elements, *Computer Methods in Applied Mechanics and Engineering*, Vol.49, No.3, 1985, pp. 357-364.

[4] Ishii M., *Thermo-Fluid Dynamic Theory of Two-Phase Flow*, Eyrolles, Paris, 1975.

[5] Chorin A. J., A numerical method for solving incompressible viscous flow problems. *Journal of Computational Physics*, Vol.2, 1967, pp.12-26.

[6] Tezduyar T. E., Mittal S., Ray S. E., and Shih R., Incompressible flow computations with bilinear and linear equal-order interpolation velocity-

pressure elements, *Computer Methods in Applied Mechanics and Engineering*, Vol.95, 1992, pp. 221-242.

[7] Hauke G. and Hughes T. J. R., A comparative study of different sets of variable for solving compressible and incompressible flows, *Computer Methods in Applied Mechanics and Engineering*, Vol.153, 1988, pp. 1-44.

[8] Thompson C. P. and Lezeau P., A novel solution algorithm for incompressible, multi-phase viscous flows, *International Journal for Numerical Methods in Fluids*, Vol.28, 1998, pp.1217-1239.

[9] Giordano M. Finite element based two-phase flow. Technical Report PR 2003-14, von Karman Institute, 2003.